

NUMERICAL INVESTIGATION OF BLADE TIP LOSS EFFECT ON THE TORQUE OF H-ROTOR VERTICAL-AXIS WIND TURBINE

Chun Khai Tan¹, Ahmad Faiz Mohammad^{*1}, Nurizzatul Atikha Rahmat², Sheikh Ahmad Zaki¹, and Farah Liana Mohd Redzuan¹

¹Malaysia-Japan International Institute of Technology, Universiti Teknologi Malaysia, Jalan Sultan Yahya Petra, 54100 Kuala Lumpur, Malaysia

²Faculty of Mechanical and Automotive Engineering Technology, Universiti Malaysia Pahang Al-Sultan Abdullah, 26600 Pekan, Pahang, Malaysia

Article history

Received

22nd February 2024

Received in revised form

16th April 2024

Accepted

8th April 2024

Published

1st June 2024

*Corresponding author
ahmadfaiz@utm.my

ABSTRACT

This research evaluated the effects of blade tip loss on H-Rotor Vertical-Axis Wind Turbines (VAWTs) and focused on elucidating the phenomenon of flow separation around a blade tip. Flow separation around the blade tip is crucial in blade tip vortex formation. This separation leads to the generation of concentrated vorticity at the blade tip, ultimately giving rise to blade tip vortices. Blade tip vortices can significantly influence the power efficiency of a VAWT. In-depth understanding of flow separation mechanisms and vortex dynamics is important for optimizing a VAWT's performance. The study is conducted via three-dimensional (3D) Computational Fluid Dynamics (CFD) using the Improved Delayed Detached Eddy Simulation (IDDES) turbulence model. Multiple test cases are employed featuring different grid densities and time step sizes, facilitating a comprehensive investigation into simulation accuracy. Key performance metrics, including the instantaneous full blade torque coefficient and the instantaneous span-wise torque coefficient, are compared. It is found that the mid-span of the blade possesses the highest torque coefficient which gradually decreases towards the blade tip, indicating the performance degradation due to blade tip loss. The study also demonstrates the effectiveness of IDDES in capturing the formation and behaviour of blade tip vortices. By comparing simulation results with experimental data, the research affirms the capability of IDDES to reproduce complex vortex dynamics within H-Rotor VAWTs. In summary, the presence of blade tip vortices was shown to degrade the generated torque of H-Rotor VAWTs

towards the blade tip. Utilizing the IDDES turbulence model and a systematic approach to mesh and time step selection underscores the importance of accurate simulation in optimizing the VAWT's performance. The findings pave the way for more precise design and operation of these complex wind energy systems, with implications for improved energy efficiency.

KEYWORDS

Blade tip loss; H-rotor vertical-axis wind turbine; computational fluid dynamics

INTRODUCTION

There is a growing interest in Vertical-Axis Wind Turbines (VAWTs) for wind energy harnessing, driven by their unique design characteristics. In general, VAWTs can be categorized into two main types: drag-type and lift-type wind turbines. The drag-type turbines generate power by harnessing wind energy through the creation of drag forces acting on their blades. In contrast, lift-type wind turbines utilize the generation of lift forces on their blades to capture wind energy. The lift-type turbines are better in power efficiency and have a broader operational range of the tip speed ratios (TSR) defined as the ratio between the wind speed and the speed of the tips of the wind turbine blades [1, 2]. The H-rotor VAWT is the most popular lift-type VAWT due to its relatively simple blade geometry [3, 4]. Therefore, it becomes a compelling option for energy harnessing in the urban environment [5, 6].

In recent years, many studies on the H-rotor VAWTs have been conducted experimentally and numerically. It has been reported that two-dimensional models exhibit significant disparities when compared to experimental findings, particularly in relation to the torque coefficient, C_m [7-9]. This discrepancy has been attributed to a three-dimensional (3D) phenomenon known as blade tip loss [9-12]. Near the blade tips, the wind flow behaves differently compared to the inner span of the blade. At the tip region, the wind flow experiences complex aerodynamic effects including flow separation, vortex shedding, and increased turbulence. As the wind flows over the blade, it undergoes acceleration on the pressure side and deceleration on the suction side. The variation in the flow velocity creates regions of differential pressure. This pressure difference induces flow separation near the blade tip, leading to the generation of blade tip vortices [13]. Blade tip vortices extract kinetic energy from the wind stream, hence, reducing the amount of energy available to the blades. This phenomenon contributes to energy loss, and as such, blade tip loss reduces the power efficiency of H-rotor VAWTs.

Blade tip vortices are relatively small in scale and highly transient, and capturing them in experiments requires expensive and specific instrumentation. With the advancement of computing power and numerical algorithms, computational fluid dynamics (CFD) becomes a useful tool in studying of these phenomena. CFD not only offers robust reliability in capturing flow patterns but also provides multi-dimensional visualizations that enrich the understanding and

interpretation of the complex flow behaviour around wind turbines [11, 14]. The Reynolds-Averaged Navier-Stokes (RANS) is one of the commonly used turbulence models in CFD analysis for VAWTs [15]. However, Lei et al., [16] reported that the Improved Delayed Detached Eddy Simulation (IDDES) turbulence model had higher accuracy than RANS. The IDDES turbulence model has the capability to capture complex, unsteady, and turbulent flow characteristics due to the integrated elements of both Large Eddy Simulation (LES) and Reynolds-Averaged Navier-Stokes (RANS) modeling [11, 17, 18].

The objective of this study is to utilize the capabilities of CFD for conducting comprehensive 3D simulations on H-rotor VAWTs. This research is focused on investigating the blade tip loss of the wind turbine and shedding light on the flow field in proximity to the blade tips. A critical aspect of this research involves the selection of an appropriate grid resolution and time step size for the IDDES turbulence model. The findings from this study carry substantial significance, offering invaluable insights to drive improvement in the power efficiency of H-rotor VAWT.

METHODOLOGY

In this study, an H-rotor VAWT model from Li et al., [9] was used and set to operate at the tip speed ratio of 2.29. The evaluation process is illustrated in Figure 1.

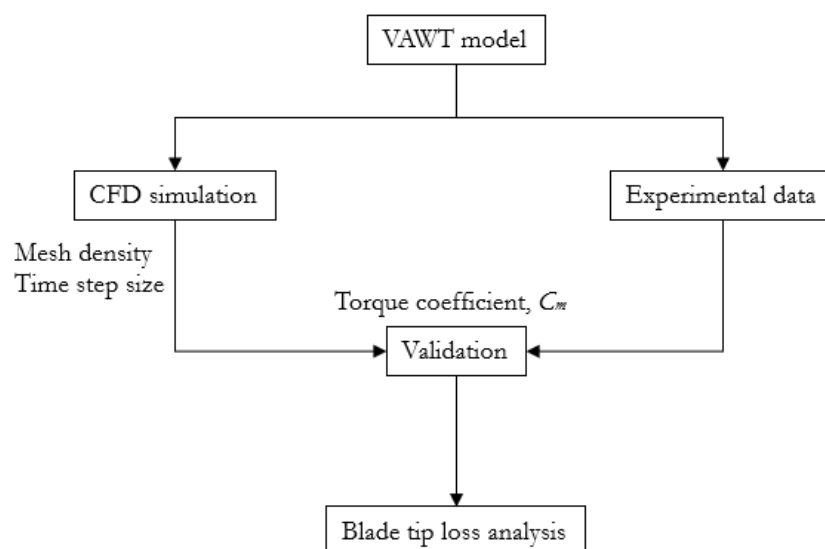


Figure 1: Evaluation process

VAWT model and operational parameters

The geometrical specification of the VAWT is shown in Table 1. The VAWT model used is a two-bladed rotor with a rotor diameter (D) of 1.7 m that uses NACA 0015 as the blade profile with a chord length (c) of 0.225 m, a blade span of 1.02 m, and $+6^\circ$ blade pitch angle. Figure 2 shows the configuration of the 3D CFD model.

In the CAD modeling, the same strategy has been applied as illustrated in the literature where the tower and support struts were excluded and only half height of the blade was modeled [9]. This

is the recommended approach to reduce the computational effort [19].

Table 1: Specifications of the H-rotor VAWT.

Parameter	Value
Airfoil	NACA 0015
Chord length, c	0.225 [m]
Blade span, H	1.02 [m]
Number of blades, N	2
Rotor diameter, D	1.7 [m]
Blade pitch	$+6^\circ$
Freestream velocity, U_∞	7 [m/s]
Parameter	Value
Airfoil	NACA 0015
Chord length, c	0.225 [m]

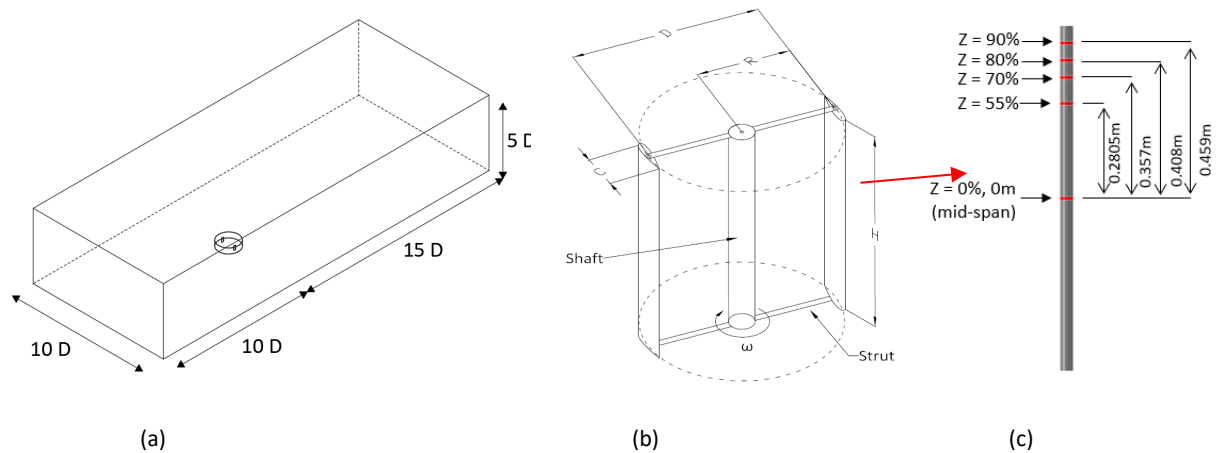


Figure 2: Configuration of the 3D CFD simulation (a) Computational domain (b) Geometrical illustration of the VAWT (c) Measurement positions.

Computational settings

The computational domain consists of two sections: the rotor and the stator. As depicted in Figure 2(a), the stator region took the form of a rectangular tunnel with dimensions of $10D$ (width) \times $5D$ (height) \times $25D$ (length), while the rotor region is a cylindrical shape with a diameter of $2.5D$ and a height of 1.02 meter. The rotor was positioned with a $10D$ upstream distance from the inlet and a $15D$ downstream distance from the outlet. At the inlet boundary, an inlet velocity (U_∞) of 7 m/s was specified, and the outlet boundary was set at a pressure condition of 0 Pa. The other four boundaries of the stator were set as symmetry conditions. The surfaces between the stator and rotor were set as an interface boundary to ensure smooth flow interaction. Finally, a no-slip wall boundary condition was used on the blade surfaces.

The entire computational domain was meshed using structured mesh topology to reduce the computational effort and increase the simulation

accuracy for the boundary layer separation. In line with well-established practices outlined in existing literature, the dimensionless wall distance (y^+) is maintained to be less than 1 [19]. This criterion adequately accounts for the effects within the viscous sub-layer boundary layer. The first cell thickness along the blade walls was set to be 1×10^{-5} meters with a growth rate set at 1.2. Overview of the mesh grid distribution around the blade is depicted in Figure 3. The sliding mesh technique was applied to allow the exchange of mass and momentum between the stator and rotor domains.

The simulation convergence is determined by analyzing the time history of the VAWT's torque coefficient, C_m , over one revolution. The calculation of C_m is defined in Equation 1 where T represents the torque generated, ρ is the air density, R is the rotor radius, and A is the swept area (VAWT's diameter multiple with the VAWT's height) of the VAWT. Convergence is achieved when the difference in the C_m between two successive revolutions is less than 1%.

$$C_m = \frac{T}{0.5\rho ARU_\infty^2} \quad (1)$$

Method for Pressure-Linked Equations) algorithm is employed to solve the fluid flow equations.

In these CFD simulations, the IDDES turbulence model is applied and the SIMPLE (Semi-Implicit

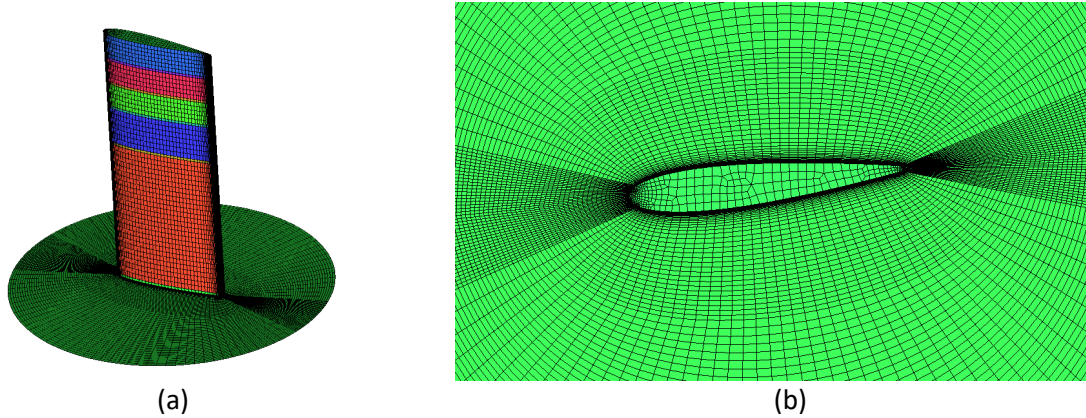


Figure 3: Computational grid distribution in the blade region (a) Mesh on the blade surface (b) Detailed grid around the blade wall.

RESULTS AND DISCUSSIONS

Ensuring the reliability of numerical models is a fundamental step in simulation studies. Verification was done by examining the mesh density and time step size. These verifications were done by comparing with the experimental data to confirm the accuracy of the numerical models. Using the established setting, blade tip loss on the wind turbine was analysed.

Simulation validation

Simulations were performed on three mesh densities which are M1, M2, and M3 by varying the number of elements around the blade as summarized in Table 2.

Table 2: Mesh densities for the simulated cases.

	M1	M2	M3
Nodes on the blade profile	176	226	276
Total number of elements	6322934	7499736	9096984

The results of the blade peak C_m (i.e. maximum torque coefficient for one blade in a complete cycle) were compared with the wind tunnel test data published by Li *et al.* [9], as presented in Table 3. In this comparison, the peak C_m was based on the mid-span of the blade (i.e. 0% spanwise

position based on Figure 2(c)). Each of the peak C_m values obtained from the three mesh densities has a low percentage difference (< 10%) with the wind tunnel data [9], indicating that the simulation setup and the mesh are convincing in to be used in this study.

Table 3: Comparison of different mesh densities peak torque coefficient at the mid-span.

Data source	C_m	Difference, %
Experiment [9]	0.324	
M1	0.346	6.79%
M2	0.352	8.64%
M3	0.340	4.94%

Furthermore, it is worth noting that the computational efficiency and accuracy of CFD simulation are affected by the chosen time step [20]. This time step is determined with respect to the azimuthal increment associated with the rotor's rotational speed, expressed as $\Delta t = \Delta\vartheta/\omega$. To explore the optimal time step size, a series of four independent studies were conducted, employing time steps of 0.5°, 0.6667°, 0.75°, and 1°, respectively. The data is summarized in Table 4. Notably, with a denser mesh and a smaller time step size, the result will be much closer to the experimental data. Balancing the considerations of

simulation efficiency and accuracy, 1° time step size was applied in all subsequent analysis.

Table 4: Comparison of different time step sizes peak torque coefficient at the mid-span.

Data source	C_m	Difference, %
Experiment [9]	0.324	
0.5° time step	0.336	3.70%
0.6667° time step	0.339	4.63%
0.75° time step	0.340	4.94%
1° time step	0.346	6.79%

Blade tip loss

To obtain insight into the blade tip loss, the analysis of C_m was extended to the entire blade span, as depicted in Figure 4. The observed trends in the full-blade C_m are identical to the C_m of the blade mid-span but with lower values. Further evaluation of the blade tip loss was carried out by evaluating the instantaneous torque coefficient at the different positions along the blade spanwise (i.e., 0% to 90%) as illustrated in Figure 2(c). The results are presented in Figure 5. It becomes evident that the peak C_m is progressively decreasing as moving from the mid-span towards the blade tip, consequently yielding a reduced overall average value. This pronounced shift in instantaneous C_m across the full revolution cycle highlights the substantial impact exerted by blade tip loss on the overall performance of the wind turbine [9, 10].

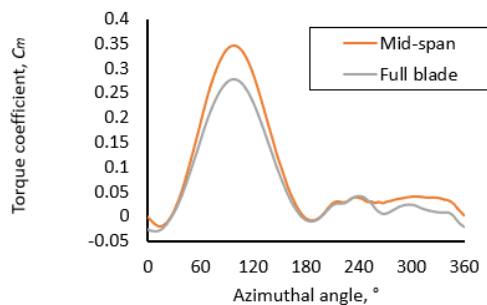


Figure 4: Comparison of the torque coefficient between the full blade and the M1 blade mid-span at full cycle.

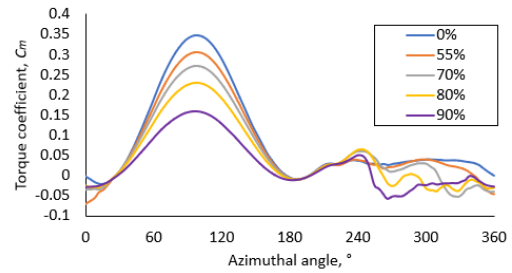


Figure 5: Single-blade instantaneous torque coefficient at five different blade span positions

The presence of blade tip vortices significantly alters the wind flow patterns around the blade, hence causing the drop in C_m [21]. As shown by the streamlines in Table 5, air near the blade tip is diverted and bypassed near the blade tip. This diversion gives rise to a swirling flow structure indicating that air particles are circulating around a central point. This circular movement represents the rotation of the blade tip vortex as illustrated in Figure 6. The streamlines in Table 5 also illustrate the inwards and upward movement of air near the vortex center, where air is being drawn in and upwards by the swirling motion.

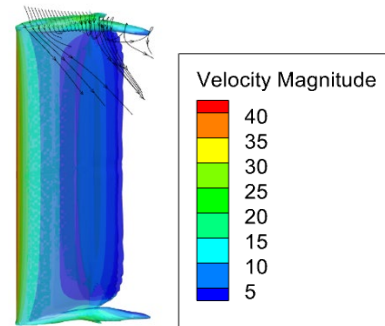
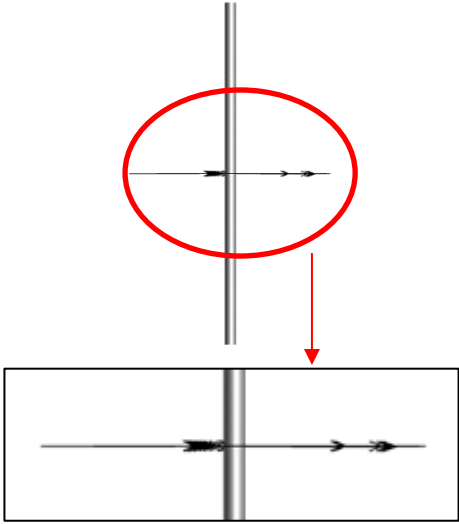
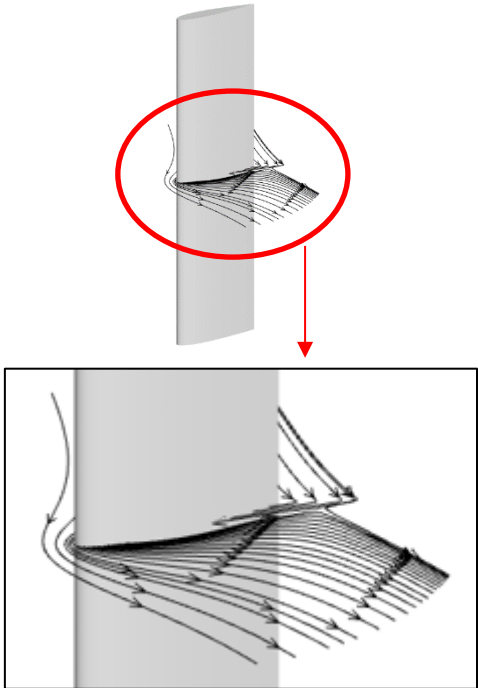
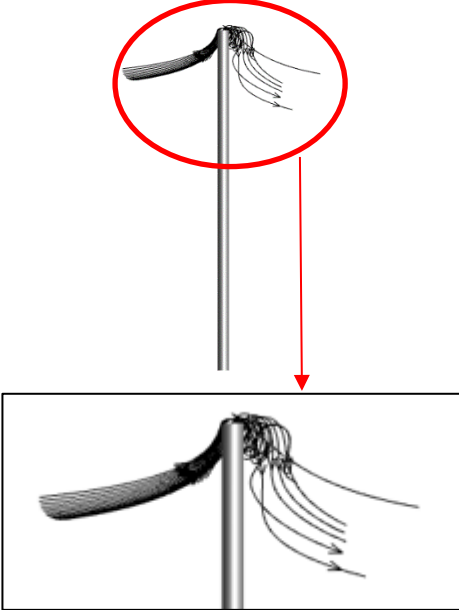
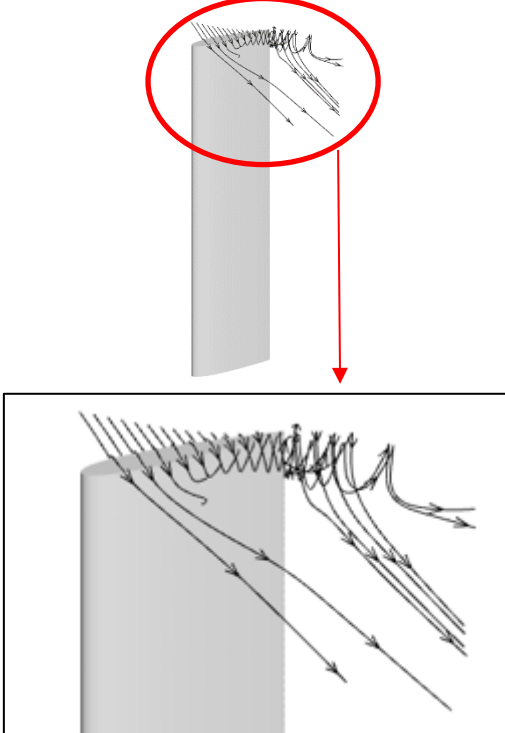


Figure 6: Vorticity iso-surface visualization.

CONCLUSION

In this paper, the application of the IDDES turbulence model to assess the blade tip loss on the H-rotor VAWT was established. A detailed analysis of how blade tip loss influences the VAWT's torque coefficient was conducted by segmenting the blade into five distinct positions. The findings revealed a gradual reduction in the torque coefficient from the mid-span toward the blade tip. While enhancing the overall efficiency of H-rotor VAWTs requires continuous investigation, future research may explore the blade tip loss under different TSRs and seek strategies for mitigating this phenomenon.

Table 5: Comparison of streamlines between the blade mid-span (0% span) and near the blade tip (90% span) at the 98° azimuthal angle from (a) perpendicular view and (b) isometric view.

Blade span position	Perpendicular view	Isometric view
0 %		
90 %		

ACKNOWLEDGEMENTS

This research was funded by the UTM-ER grant (Vot No. 20J89) of Universiti Teknologi Malaysia.

REFERENCES

- [1] Bhutta, M. M. A., Hayat, N., Farooq, A. U., Ali, Z., Jamil, S. R. and Hussain, Z., 2012. Vertical axis wind turbine – A review of various configurations and design techniques. *Renewable and Sustainable Energy Reviews*, 16(4), pp. 1926-1939.
- [2] Castelli, M. R. and Benini, E., 2011. Comparison between lift and drag-driven VAWT concepts on low-wind site AEO. *World Academy of Science, Engineering and Technology*, pp. 1677-1682.
- [3] Brownstein, I. D., Wei, N. J. and Dabiri, J. O., 2019. Aerodynamically Interacting Vertical-Axis Wind Turbines: Performance Enhancement and Three-Dimensional Flow. *Energies*, 12(14).
- [4] Gharaati, M., Xiao, S., Wei, N. J., Martínez-Tossas, L. A., Dabiri, J. O. and Yang, D., 2022. Large-eddy simulation of helical- and straight-bladed vertical-axis wind turbines in boundary layer turbulence. *Journal of Renewable and Sustainable Energy*, 14(5).
- [5] Zabarjad Shiraz, M., Dilimulati, A. and Paraschivoiu, M., 2020. Wind power potential assessment of roof mounted wind turbines in cities. *Sustainable Cities and Society*, 53.
- [6] Toja-Silva, F., Colmenar-Santos, A. and Castro-Gil, M., 2013. Urban wind energy exploitation systems: Behaviour under multidirectional flow conditions— Opportunities and challenges. *Renewable and Sustainable Energy Reviews*, 24, pp. 364-378.
- [7] Franchina, N., Persico, G. and Savini, M., 2019. 2D-3D computations of a vertical axis wind turbine flow field: Modeling issues and physical interpretations. *Renewable Energy*, 136, pp. 1170-1189.
- [8] Lanzafame, R., Mauro, S. and Messina, M., 2014. 2D CFD Modeling of H-Darrieus Wind Turbines Using a Transition Turbulence Model. *Energy Procedia*, 45, pp. 131-140.
- [9] Li, Q., Maeda, T., Kamada, Y., Murata, J., Kawabata, T., Shimizu, K., Ogasawara, T., Nakai, A. and Kasuya, T., 2016. Wind tunnel and numerical study of a straight-bladed vertical axis wind turbine in three-dimensional analysis (Part I: For predicting aerodynamic loads and performance). *Energy*, 106, pp. 443-452.
- [10] Zanforlin, S. and Deluca, S., 2018. Effects of the Reynolds number and the tip losses on the optimal aspect ratio of straight-bladed Vertical Axis Wind Turbines. *Energy*, 148, pp. 179-195.
- [11] Miao, W., Liu, Q., Xu, Z., Yue, M., Li, C. and Zhang, W., 2022. A comprehensive analysis of blade tip for vertical axis wind turbine: Aerodynamics and the tip loss effect. *Energy Conversion and Management*, 253.
- [12] Lam, H. F. and Peng, H. Y., 2016. Study of wake characteristics of a vertical axis wind turbine by two- and three-dimensional computational fluid dynamics simulations. *Renewable Energy*, 90, pp. 386-398.
- [13] Balduzzi, F., Drofelnik, J., Bianchini, A., Ferrara, G., Ferrari, L. and Campobasso, M. S., 2017. Darrieus wind turbine blade unsteady aerodynamics: a three-dimensional Navier-Stokes CFD assessment. *Energy*, 128, pp. 550-563.
- [14] Posa, A., 2020. Influence of tip speed ratio on wake features of a vertical axis wind turbine. *Journal of Wind Engineering and Industrial Aerodynamics*, 197, p. 104076.
- [15] Ghasemian, M., Najafian Ashrafi, Z. and Sedaghat, A., 2017. A review on computational fluid dynamic simulation techniques for Darrieus vertical axis wind turbines. *Energy Conversion and Management*, 149, pp. 87-100.
- [16] Lei, H., Zhou, D., Bao, Y., Li, Y. and Han, Z., 2017. Three-dimensional Improved Delayed Detached Eddy Simulation of a two-bladed vertical axis wind turbine. *Energy Conversion and Management*, 133, pp. 235-248.
- [17] Kuang, L., Lei, H., Zhou, D., Han, Z., Bao, Y. and Zhao, Y., 2021. Numerical Investigation of Effects of Turbulence Intensity on Aerodynamic Performance for Straight-Bladed Vertical-Axis Wind Turbines. *Journal of Energy Engineering*, 147(1).
- [18] Xu, W., Li, G., Wang, F. and Li, Y., 2020. High-resolution numerical investigation into the effects of winglet on the aerodynamic performance for a three-dimensional vertical axis wind turbine. *Energy Conversion and Management*, 205.
- [19] Matsson, J. E., 2023. *An Introduction to Ansys Fluent 2023*. SDC Publications.
- [20] Gritskevich, M. S., Garbaruk, A. V., Schütze, J. and Menter, F. R., 2011. Development of DDES and IDDES Formulations for the k- ω Shear Stress Transport Model. *Flow, Turbulence and Combustion*, 88(3), pp. 431-449.
- [21] Jiang, Y., He, C., Zhao, P. and Sun, T., 2020. Investigation of Blade Tip Shape for Improving VAWT Performance. *Journal of Marine Science and Engineering*, 8(3).